Journal of Hydrology: Regional Studies 53 (2024) 101760

Contents lists available at ScienceDirect

Journal of Hydrology: Regional Studies

journal homepage: www.elsevier.com/locate/ejrh

Assessing urban drainage pressure and impacts of future climate change based on shared socioeconomic pathways

Yao Li [a,b], Pin Wang [a,c,*], Yihan Lou [a,c], Chaohui Chen [a,c], Chenghua Shen [a,c], Tangao Hu [a,c]

[a] Institute of Remote Sensing and Earth Sciences, Hangzhou Normal University, Hangzhou 311121, China
[b] Faculty of Geo-Information Science and Earth Observation (ITC), University of Twente, Enschede 7500AE, the Netherlands
[c] Zhejiang Provincial Key Laboratory of Urban Wetlands and Regional Change, Hangzhou 311121, China

A R T I C L E I N F O

Keywords:
Urban drainage pressure
Urban flooding
Climate change
SWMM model
CMIP6
SSP-RCP

A B S T R A C T

The increasing frequency of urban flood disasters presents a significant obstacle to urban sustainability. Urban flood management aims to reduce the flood occurrences, currently addressed through urban drainage systems. Previous studies have demonstrated future precipitation extremes will pose larger pressure on urban drainage network, but when and where the pressure will reach a dangerous level have never been assessed in any city of China. This study establishes the initial framework for identifying critical decades and hot spots of urban drainage pressure changes due to future climate change, through a case study conducted in southern China (Haining city). Urban drainage pressure was assessed by a combination of the urban drainage model known as the Storm Water Management Model (SWMM) and pipe statistics. Using climate projections from the latest phase of Coupled Model Intercomparison Project (CMIP6) under four typical SSP-RCP (shared socioeconomic pathway-representative concentration pathway) scenarios, we project the changes in urban drainage pressure by 21st century, and identify the key decades and high risk areas with the occurrence of dangerous pressure levels. The results indicate an overall upward trend in urban drainage pressure for Haining city, with over 97% of the flooding nodes projected to firstly reach the dangerous level by the 2030 s. Comparisons of the patterns under different SSP-RCP scenarios, suggest that a higher forcing pathway would expedite the deterioration of urban drainage pressure, particularly in urban areas with lower DEM and high building intensity. This has broad implications for better informing disaster management and policy-making in similar cities, especially those with inadequate drainage capacities.

1. Introduction

Urban flooding has posed devastating impacts on society and city infrastructure (Blöschl et al., 2019; Depietri and McPhearson, 2018; Liu et al., 2023; Tellman et al., 2021). During 2011–2014, approximately 62% of surveyed Chinese cities experienced flood-related damages, resulting in direct economic losses amounting to around USD 100 billion (China Statistical Yearbook, 2015; Zhou et al., 2018). With the rapid urbanization urban flooding occurred more frequently over recent decades (Li et al., 2022; Luo and Zhang, 2022; Tang et al., 2024). Global-scale climate change would affect precipitation pattern in most of China, resulted in more

* Corresponding author at: Institute of Remote Sensing and Earth Sciences, Hangzhou Normal University, Hangzhou 311121, China.
E-mail address: wangpin@hznu.edu.cn (P. Wang).

https://doi.org/10.1016/j.ejrh.2024.101760
Received 8 October 2023; Received in revised form 11 January 2024; Accepted 27 March 2024
Available online 5 April 2024
2214-5818/

precipitation extremes in the upcoming period (Dawkins et al., 2022; Moustakis et al., 2021; Zhai et al., 2020). That poses a major challenge to execute urban flood management strategies in most cities. Typically, these strategies involve the utilization of the drainage system including the pipes and manholes (Gimenez-Maranges et al., 2020; Li and Bortolot, 2022). Hence, assessing the changes of urban drainage pressure is of significant importance for proactive policymaking and offering long-term insights into urban disaster management.

In the previous studies, numerous models have been developed to simulate the hydrologic processes during storm events (Farina et al., 2023; Lou et al., 2024). These include Storm Water Management Model (SWMM), InfoWorks, Hydrologic Simulation Program Fortran, and MIKE FLOOD. These models have been used to simulate the impacts of extreme precipitation events on the overflow volume or flood inundation condition (Son et al., 2023; Yang et al., 2021). It was found that urban flood risk would significantly increase under future climate change (Kim et al., 2017; Wasko et al., 2021). Generally, the design of drainage systems relies heavily on historical precipitation statistics for a specific time period, disregarding the potential variations in extreme precipitation events. Given these facts, it becomes crucial to assess the impact of future climate on urban flood pressure caused by precipitation extremes. However, there is currently a gap in simulations addressing urban drainage pressure under future climate change, especially in the cities struggling with substantial drainage capacity constraints.

Currently, coordinated climate model intercomparison which enabled by the Coupled Model Intercomparison Project (CMIP), was used to derive global precipitation projections (Chen et al., 2020; NCC-Editorial, 2019; Xu et al., 2022). Based on the outputs from the CMIP models, future changes of precipitation extremes throughout China have been assessed (Tian et al., 2021; Xu et al., 2022). Given the uncertainties in social development and emission scenarios during the future period (Heinze et al., 2019; NCC-Editorial, 2019), the improved climate projections recently published by CMIP6 (CMIP is in its sixth phase) could help obtain more robust estimations (Cos et al., 2022; Eyring et al., 2016). Under the SSP-RCP (shared socioeconomic pathway-representative concentration pathway) scenarios of 2–4.5 and 5–8.5, substantial increases in maximum 5-day precipitation and the occurrence of very heavy precipitation days are predicted across China in the coming decades (Xu et al., 2022). Considering the drainage system's capacity, Lu et al. (2018) and Wang et al. (2023) revealed the changes in urban drainage pressure under future climate change. They found that more than 90% of China's major cities would see larger pressure in this century. Some typical cities have been chosen to illustrate the increases of urban flood volume and inundation area during the future period (Sun et al., 2021; Zhou et al., 2018, 2019).

Based on these findings, several studies have further discussed the effects of local adaptation by modifying drainage systems to cope with the increasing risk of urban flooding (Sun et al., 2021; Wang et al., 2023; Zhou et al., 2018). For instance, SWMM was applied to assess the impact of pipe enlargement and low impact development on urban flood volumes by Zhou et al. (2018) in Hohhot city. Sun et al. (2021) employed InfoWorks Integrated Catchment Modeling (ICM) to model the effects of local adaptation measures on flood volume and inundation area in central Shanghai. These researchers stressed that the drainage system adaptation measures can efficiently mitigate flooding in the 21st century. However, the implementation of such measures is often difficult, expensive, and time-consuming for city governments. Therefore, it is crucial to identify when and where the pressure will reach a dangerous level within the drainage network of a given city. This information has the potential to provide valuable guidance to local governments in

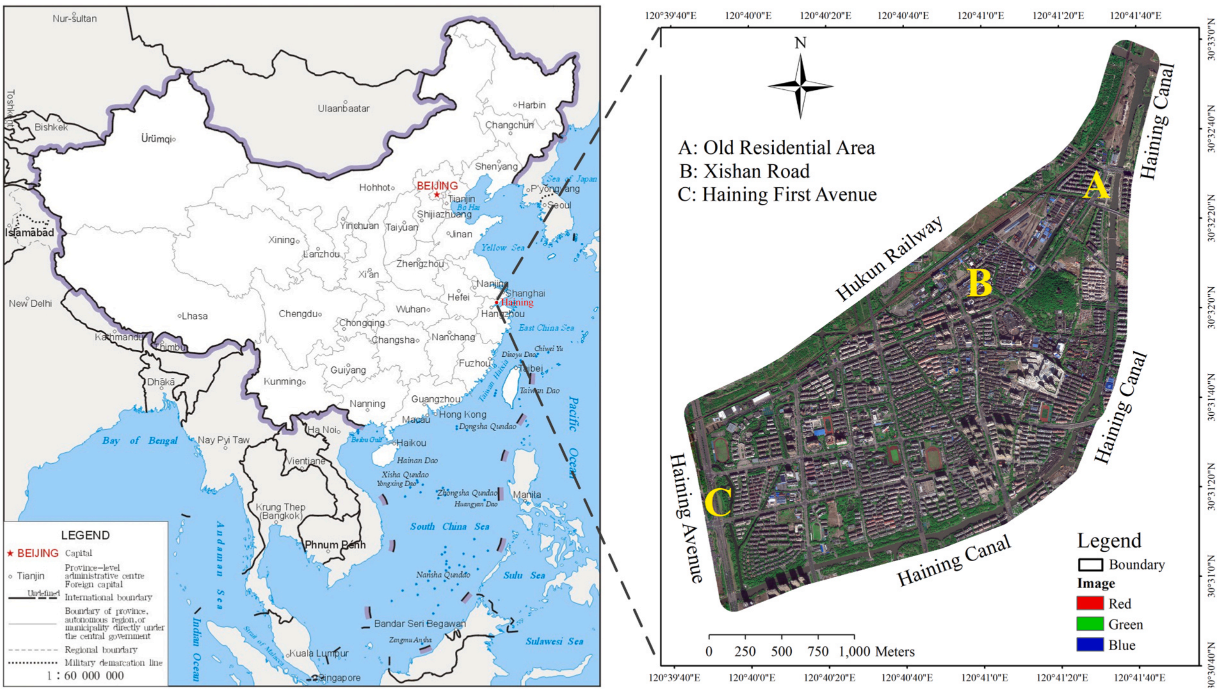

Fig. 1. Study area.

the planning of new urban drainage systems and the redesign of existing ones.

Haining city, a typical southeast coastal city in Zhejiang Province, China, is struggling with substantial drainage capacity constraints (Wang et al., 2022). Given its flat topography and rapid urbanization, Haining City relies heavily on its drainage system to manage storm rainfall. However, the current drainage system was established several decades ago and may not be equipped to handle the challenges posed by future climate change. Solving its problem could provide crucial insights for numerous cities with limited drainage capacity in China. Among the hydrologic models, SWMM introduced by the United States Environmental Protection Agency in 1971, stands out due to its numerous advantages. These include its open-source code, facilitating convenient modeling, and providing reliable calculation of pipeline discharge. These features contributed to its extensive utilization in engineering applications and academic research worldwide. For example, Zhou et al. (2018) utilized SWMM to simulate urban flood volumes and access the adaption methods; Farina et al. (2023) employed SWMM to simulate the hydrological process of urban drainage systems; and Zhuang et al. (2023) used SWMM to evaluate runoff control of low impact development.

Therefore, in this study, Haining City was taken as an example to assess the impact of future climate change on urban drainage pressure. We proposed an evaluation framework for identifying critical decades and hot spots experiencing significant changes in urban drainage pressure, utilizing shared socioeconomic pathways and CMIP6 models. Based on the simulations from the SWMM model, we aimed to: (1) assess the impacts of future climate change on urban drainage pressure throughout the 21st century; (2) identify the key time points and areas with significant change in urban drainage pressure; (3) compare the spatio-temporal patterns of urban drainage pressure under different SSP-RCP scenarios. This study has the potential to provide valuable insights into urban flood management strategies for similar cities, particularly where the drainage capacities are inadequate.

2. Materials and methodology

2.1. Study area and datasets

Haining (30°30’N, 120°40’E) is a typical southeast coastal city, located in Zhejiang Province, China (Fig. 1). It is a highly urbanized area with the relatively low terrain and density impervious area, which makes it easy to be influenced by frequent urban flooding disasters during rainy season. Urban flooding has become a critical issue according to China’s first general survey of natural disasters. Therefore, the drainage system of Haining city is under high pressure with the dramatic climate change. The central region of Haining was selected as study area, given its pivotal significance in Haining. This area is 5.9 km^2 with dimensions of 2.7 km long and 2.2 km wide. The total length of the pipelines in the system is 58.4 km. The drainage system in the area is outdated, having been constructed five decades ago, and is now inadequate for the current drainage needs (Li et al., 2019). Given that Haining is a highly urbanized city in southeastern China, studying the changes in urban drainage pressure under climate change holds significant practical importance. For the urban drainage pressure simulations and climate change assessments, we collected Digital Elevation Model (DEM) (Fig. 2a), remote sensing image, land use (Fig. 2b), urban drainage network (Fig. 2c), and meteorological data. The data sources and related information can be found in Table 1.

2.2. Future precipitation calculation

2.2.1. CMIP6 dataset

The observed data of daily precipitation were obtained by interpolating data from 2472 meteorological stations (http://data.cma.cn/site/index.html) across China between 2000 and 2014. The future precipitation projections were sourced from five CMIP6 models known for their robust performance in simulating extreme precipitation events within the Chinese region (Table 2). The projections

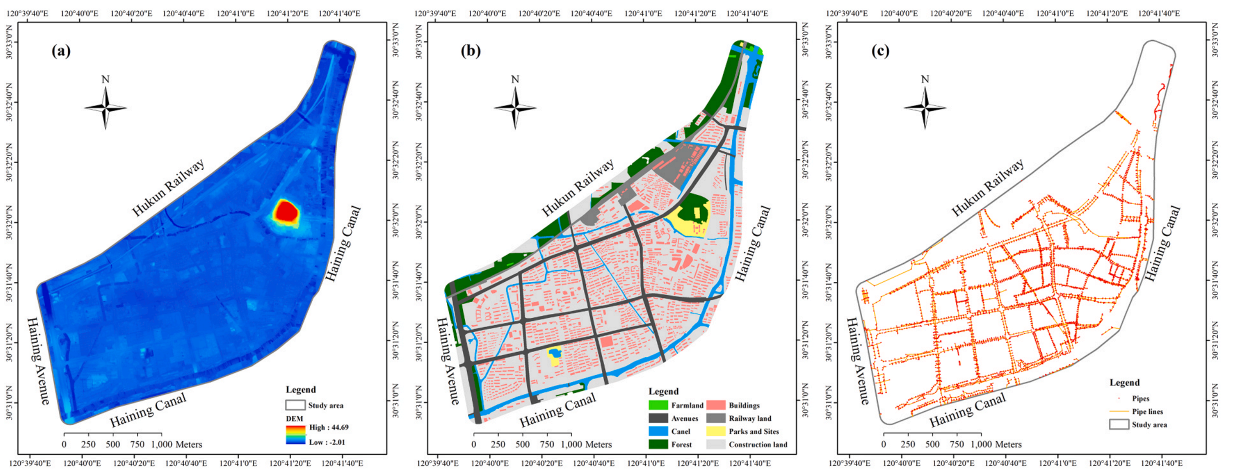

Fig. 2. Overview of the datasets: (a) DEM, (b) land cover, and (c) urban drainage network.

Table 1
List of datasets used in this study.

Data	Format	Resolution	Source
DEM	Raster	2 m	Zhejiang Administration of Surveying Mapping and Geoinformation
Unmanned aerial vehicle (UAV) image	Raster	0.5 m	
Land cover survey data	Shapefile	Polygon	Haining Natural Resources Bureau
Urban drainage network	Shapefile	Line/Point	Haining Drainage Management Bureau
Meteorological records	Text	min	Haining precipitation station
Measured flow data	Text	min	Field survey

from these five models have been widely used in many research areas across China, as evidenced by studies such as Lou et al. (2024), Tian et al. (2021) and Xu et al. (2022). The assessment results have been validated as effective in depicting the interannual variability of precipitation extremes in most area of China. We only used data from the initial run of the "r1i1p1f1" model simulations.

The novel SSP-based scenarios present alternative routes to achieve varying levels of radiative forcing through diverse socioeconomic development pathways (Hou et al., 2022). Specifically, the present studies focused on analyzing four tier-1 scenarios, namely SSP1–2.6, SSP2–4.5, SSP3–7.0, and SSP5–8.5. The SSP1–2.6 scenario corresponds to the lower bound of future scenarios in terms of radiative forcing. According to model simulations, this scenario is expected to result in a global mean temperature increase of less than 2.0 ℃ by the year 2100. Therefore, this scenario has the potential to align with the target of limiting global warming to 2.0 ℃ as proposed in various studies (O'Neill et al., 2016; Tebaldi et al., 2020). The SSP2–4.5 scenario is categorized as a moderate stabilization scenario, whereas the SSP3–7.0 scenario represents a pathway with moderate-to-high levels of radiative forcing. And the SSP5–8.5 scenario is a high radiative forcing pathway in which radiative forcing is stabilized at 8.5 Wm-2 in 2100 (Tebaldi et al., 2020).

2.2.2. Precipitation index calculation

We have analyzed the historical trend of extreme precipitation in Haining city and found a significant increase in the intensity of extreme precipitation since 1990. In order to reflect urban drainage pressure caused by heavier flooding, we selected a relatively severe period (1990–2014) and chose the maximum daily precipitation for each year. Considering that the CMIP6 model takes 2014 as the end point for simulating historical periods, we calculated the index during 1990–2014 as the historical level. Utilizing precipitation data from 1990 to 2014, we implemented the Equidistant Cumulative Distribution Functions (EDCDF) method to correct the bias in the unadjusted outputs from the CMIP6 models (Guo et al., 2020; Piao et al., 2022; Wang and Chen, 2013). In general, the precipitation simulation results for China during the historical period showed a strong agreement with the observed precipitation data, in accordance with the findings presented in the study conducted by Tian et al. (2021). Therefore, we performed bias correction on all CMIP6 model data hereafter presented in this study. Annual maximum precipitation during a given period was averaged as the extreme precipitation index, which serves as a useful indicator of extreme precipitation events that a city may experience. Considering the significant inter-annual variation in precipitation extremes, the extreme index was calculated for each decade in the future period. Multi-model ensemble estimates were used to address the inter-model variability in future precipitation projections.

2.2.3. Precipitation event determination

The Chicago Design Storm (CDS) formula, as a well-established approach for temporal downscaling of daily precipitation data to finer time scales, has been widely employed in numerous studies related to flood simulation and urban storm drainage design (Bibi, 2022; Li et al., 2020; Wetterhall et al., 2006). The Engineering Construction Standards of Zhejiang Province: *Urban Flood Prevention Planning Standard Profile* from the Housing and Urban-Rural Development Department of Zhejiang Province (https://jst.zj.gov.cn/) provided us with the CDS distribution pattern. This pattern was derived from 44 years of recorded rainfall data from 1963 to 2006, where the calculation of the annual maximum value and year-to-sample method was carried out using the Gumbel-type function curve method for compilation. The CDS distribution of future precipitation events will serve as the rainfall inputs for the following urban drainage model, with a duration of 120 minutes, a step of 5 minutes, and a rain peak coefficient of 0.4.

Table 2
List of five CMIP6 models used in this paper and their spatial resolution.

Model	Country	Resolution (Lon × Lat)	Leap year
BCC-CSM2-MR	China	1.125° × 1.1°	NO
CanESM5	Canada	~2.8° × ~2.8°	NO
IPSL-CM6A-LR	France	2.5° × ~1.3°	YES
MRI-ESM2–0	Japan	1.125°× ~1.1°	YES
MIROC6	Japan	~1.4° × 1.4°	YES

2.3. Urban drainage modelling

2.3.1. Model construction

The Storm Water Management Model (SWMM) known as a dynamic rainfall-runoff model, was developed by the United States Environmental Protection Agency (USEPA) in 1971. This model was often used to simulate the quantity and quality of runoff from primarily urban areas, both for single events and long-term simulations (Zhu et al., 2023). One of the model's notable features is its ability to estimate the volume of floodwater in the drainage system, which shows advantages for urban runoff simulation (Zhou et al., 2018). Its versatility and accuracy have made it widely adopted for planning, analysis and design related to drainage systems in urban areas (Li et al., 2019). When the surface runoff volume exceeds the sewer pipe's capacity, overflow may occur, and the flood volume over the manhole can indicate the urban drainage pressure. This can place a significant hydraulic burden on the urban drainage system.

For hydrological process, the study area was divided into 1368 sub-catchments and the physical characteristics of sub-catchments, such as areas, overland flow path widths, and impervious rate were calculated as the input based on DEM and land use map. The Infiltration module are based on Soil Conservation Service curve number (SCS-CN) method. The governing equation (Rossman, 2015) equals:

$$\frac{\partial d}{\partial t} = i - e - f - \frac{WS^{\frac{1}{2}}}{A_s n}\left(d - d_p\right)^{\frac{5}{3}} \tag{1}$$

where d is water depth (m), t is time (s), i is the rate of rainfall (ms^{-1}), e is the rate of evaporation (ms^{-1}), f is the rate of infiltration (ms^{-1}), W is width of the sub-catchment (m), n is surface roughness coefficient, S is average slope of the sub-catchment, A_s is surface area of the sub-catchment (m^2), d_p is depression storage depth (m).

During the hydraulic process, the parameters for conduits, junctions and manholes, including shape, length, diameter, and spatial position can be obtained from the pipe dataset. The kinematic wave and the Saint-Venant equations were utilized for hydraulic simulations in this study to get the flow routing results (Rossman and Huber, 2016). The hydraulic flow is obtained by the St. Venant equation (Rossman, 2015):

$$\frac{\partial Q}{\partial t} + \mathrm{gA}\frac{\partial \mathrm{H}}{\partial x} + \mathrm{gA}S_f - 2v\frac{\partial A}{\partial t} - v^2\frac{\partial A}{\partial x} = 0 \tag{2}$$

where Q is flow rate (m^3s^{-1}), t is time (s), g is gravity (ms^{-2}), A is flow cross-sectional area (m^2), H is hydraulic head of water in the conduit (m), x is distance (m), S_f is friction slope, and v is flow velocity (ms^{-1}).

2.3.2. Model calibration and validation

To ensure the model better reflect the real-world scenarios, two historical rainfalls (29 May 2020 and 2 July 2020) were used to calibrate the model and another rainfall event (21 July 2021) were used for model validation. Nash-Sutcliffe efficiency coefficient (NSE) was employed to assess model performance (Bal et al., 2021). The NSE equation is as follows:

$$NSE = 1 - \frac{\sum_{i=1}^{n}\left(O_i - S_i\right)^2}{\sum_{i=1}^{n}\left(S_i - O_{avg}\right)^2} \tag{3}$$

where O_i is the observed value at the i^{th} timestep; S_i is the model simulated value at the i^{th} timestep; O_{avg} is the average of the observed values. The NSE ranges from -∞ to 1, with values closer to 1 indicating better performance. Generally, NSE values exceeding 0.5 are considered to meet the accuracy evaluation criteria for hydrological models (Lisenbee et al., 2022; Zhang and Li, 2015; Zhuang et al., 2023).

2.4. Analysis

The flooding nodes and volume caused by a given precipitation extreme can be simulated by the SWMM. Urban drainage pressure will be reflected from two aspects: the total number of flooding nodes (TFN) and the total flooding volume (TFV) in study area. The mean value of TFV during 2000–2014 was computed as the TFV baseline level. Meanwhile, we proposed the urban drainage pressure index (UDPI) to access the urban drainage pressure:

$$UDPI = \frac{\mathrm{FV}}{\mathrm{PC}} \tag{4}$$

where FV (m^3) is flood volume, PC (m^2) is the pipe cross-sectional area. We evaluated the urban drainage pressure during each decade (2020 s, 2030 s, 2040 s, 2050 s, 2060 s, 2070 s, 2080 s, and 2090 s) under four SSP-RCP scenarios (SSP1–2.6, SSP2–4.5, SSP3–7.0, and SSP5–8.5).To assess the temporal trends of the entire study area under future climate change in the 21st century, the linear regression method was employed to analysis the changing trends of TFV. Subsequently, we compared the UDPI of each node under different SSP-RCP scenarios with the baseline. If the UDPI of a node increased by over 30% of the baseline, we considered it to have reached dangerous pressure levels. The occurrence and duration of these dangerous pressure levels were then analyzed to identify the critical decade and high risk area of the urban drainage pressure changes. This can provide suggestions for flooding mitigation management. The overall workflow is shown in Fig. 3.

3. Results

3.1. Temporal changes of precipitation extremes under different SSP-RCP scenarios

Future precipitation calculation indicated that different SSP-RCP scenarios would result in varying trends in precipitation extremes (Fig. 4). SSP1–2.6 predictions would show no significant trend in precipitation extremes between the 2020 s and 2050 s, followed by a decreasing trend from the 2060 s onwards. For SSP2–4.5, precipitation extremes were expected to increase from the 2020 s to 2050 s, reach a peak in the 2070 s, and then gradually decrease. In contrast, SSP3–7.0 would foresee a positive trend in precipitation extremes since the 2040 s. Under SSP5–8.5, the increase in precipitation extremes would be highly significant. The maximum precipitation would range from 70 mm to 90 mm.

3.2. Performance of SWMM

Following the calibration process, the parameter settings for SWMM are as follows: *N-Imperv* is set as 0.031, *N-Perv* is set as 0.59, *Destore-Imperv* is set as 6.5, *Destore-Perv* is set as 5, *Zero-Imperv* is set as 38, *Maxrate* is set as 56, *Minrate* is set as 2.09, and *Decay* is set as 28. These values were determined through the and have improved the model's performance and accuracy. In this study, the NSE reached 0.76 during validation, indicating a good agreement between the model predictions and the observed data.

3.3. Urban drainage pressure changes under different SSP-RCP scenarios

3.3.1. Temporal Changes of total flood volume

The impacts of precipitation extremes on urban drainage pressure in the 21st century are highlighted in Fig. 5, examining four

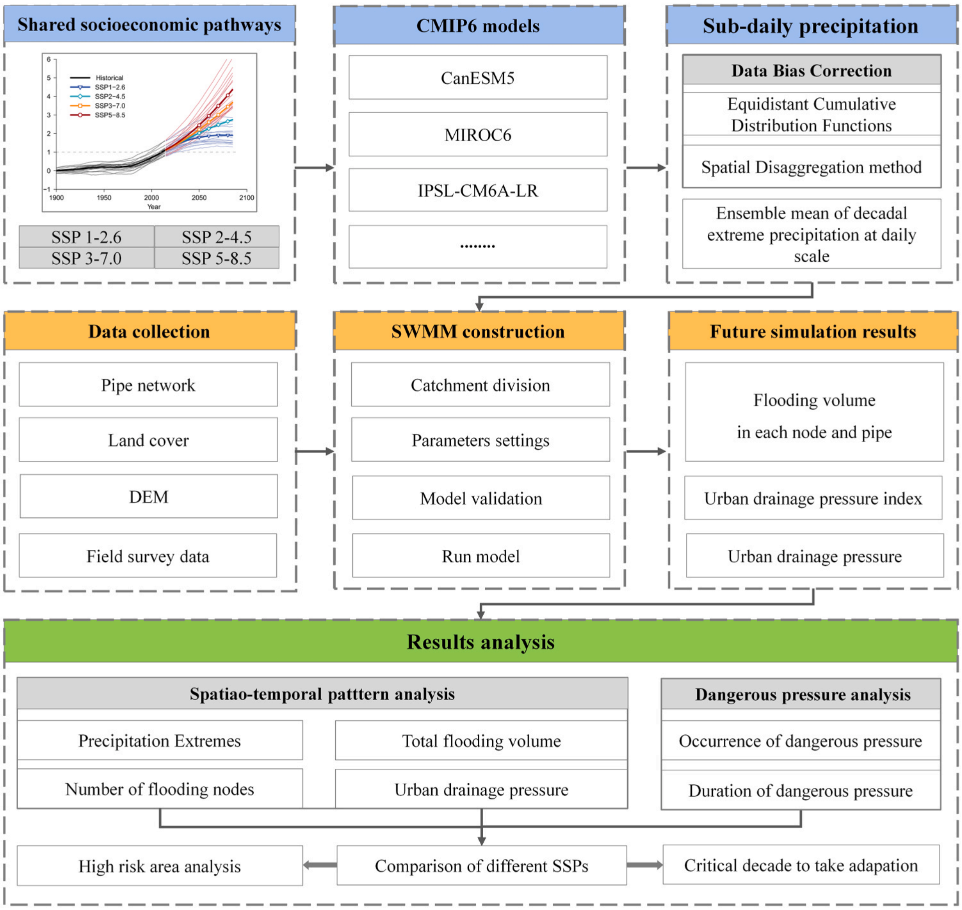

Fig. 3. Overall workflow of this study.

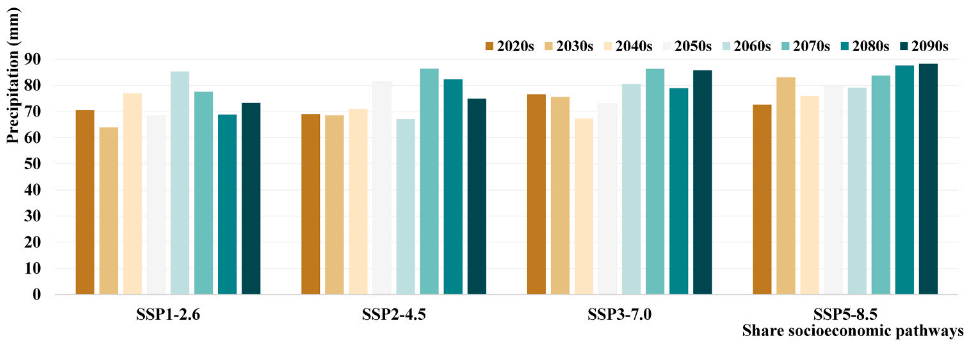

Fig. 4. Temporal changes of precipitation extremes from the 2020 s to 2090 s under each SSP-RCP scenario.

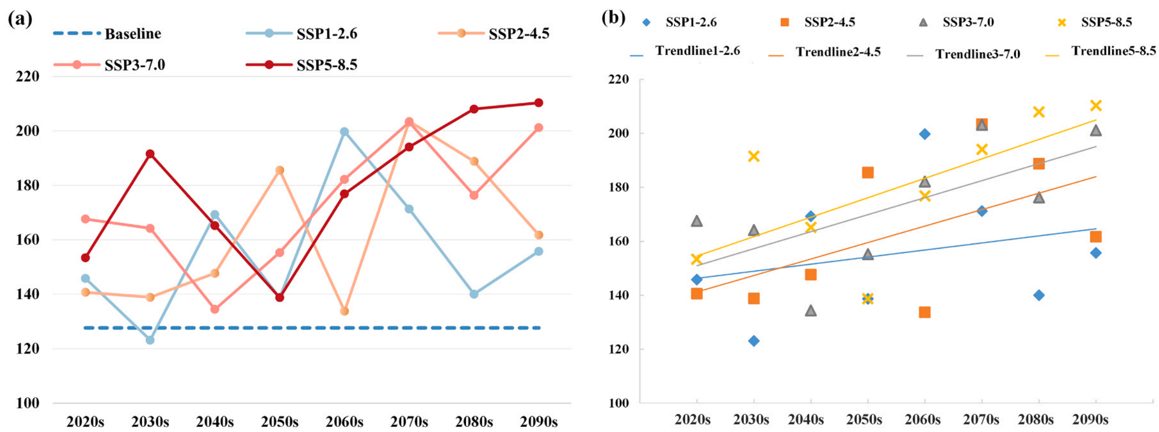

Fig. 5. The changes of TFVs under four SSP-RCP scenarios in the 21st century (Unit: 10^3 m^3): (a) the changing line, (b) linear trend line.

different SSP-RCP scenarios based on the current drainage system. Considering the TFV under four SSP-RCP scenarios, urban drainage pressure is observed to fluctuate over time (Fig. 5a), but with an overall upward trend (Fig. 5b). Among all the changes, SSP5–8.5 scenario has emerged as the fastest-growing trend, and the maximum TFV (210343 m^3) would appear in the 2090s under the SSP5–8.5 scenario.

3.3.2. Changes of urban flood pressure relative to baseline level

Under four SSP-RCP scenarios, as shown in Fig. 6, the UDPI would increase significantly throughout the study area compared with the baseline at the end of the 21st century (2090s). Spatially, the urban drainage pressure will mainly affect the road and avenues. Under SSP1–2.6 scenario, the most severe drainage pressure would show in the Xishan road, and the UPDI was expected to increase by a factor of 11 compared to the baseline level (Fig. 6a). As shown in Fig. 6b, the severe flooding volume would gradually show in Haining First Avenue, Wenzong road and Wenyuan road. There has been a dramatic increase of UPDI compared with baseline. At the end of the century, in 2090s, the northern part of Xishan road would be the most severe area. The maximum flooding volume would overflow in the north part of Yujiaqiao street. Other severe points would occur on the Youquan road and Xishan road. As shown in Fig. 6d, the UPDI under scenario SSP5–8.5 in 2090s is almost twice as large as baseline.

Although some changes were observed for TFN, they were not statistically significant, and the total number of flooding points remained relatively stable. Considering the TFN exceeding dangerous levels (TFN-D) in Fig. 7, under the SSP1–2.6 scenario, the TFN-D would stay in a fluctuating state, where the highest peak would happen in the 2060s, which is approximately 25% of the total node numbers in Haining. Under the SSP2–4.5 scenario, the TFN-D would dramatically increase from 2070s and the maximum value would appear in 2070s. Under the SSP3–7.0 scenario, the TFN-D would significantly increase since the 2060s. Under SSP5–8.5 scenario, there is a peak in the 2030s and about 25% nodes would in dangerous level during the second half of this century.

3.4. Occurrence of dangerous pressure level under different SSP-RCP scenarios

3.4.1. Changes in the first occurrence of dangerous pressure

The simulation results indicated that Haining's urban drainage pressure would first surpass the dangerous level during the 2040s under the SSP1–2.6 scenario. Under the SSP2–4.5 and SSP3–7.0 scenarios, the first occurrence of dangerous levels would be expected in 2050s and 2020s, respectively. Under the SSP5–8.5 scenario, the dangerous level would start since 2030s until the end of the

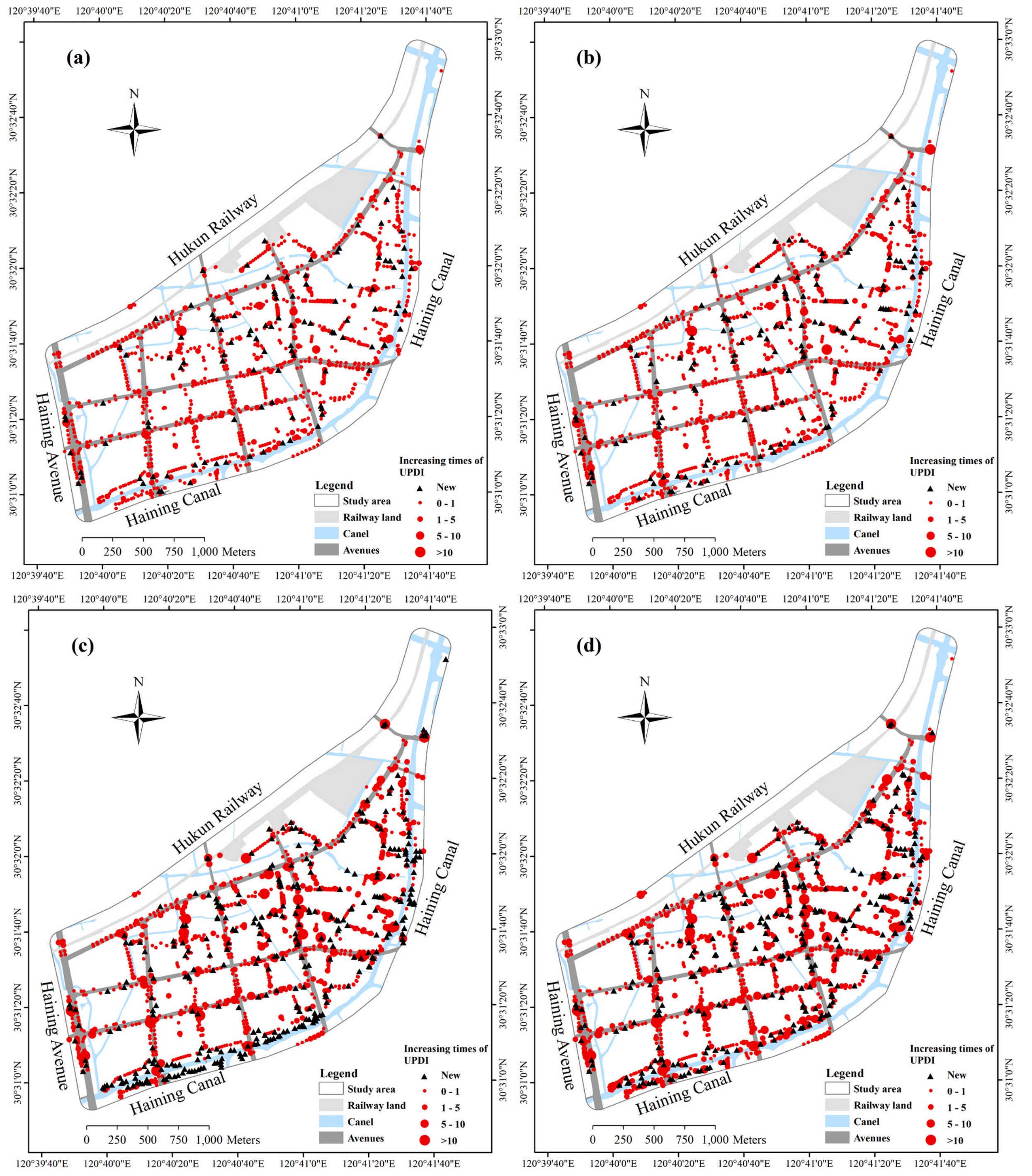

Fig. 6. The increasing times of UPDI relative to baseline level in 2090 s under four SSP-RCP scenarios: (a) SSP1-2.6, (b) SSP2-4.5, (c) SSP3-7.0, (d) SSP5-8.5.

century, which would happen in five decades and continue 40 years from 2060s.

Fig. 8 illustrates the changes in the occurrence of dangerous pressure, with earlier occurrences indicating greater pressure levels. Under SSP1–2.6 scenario, approximately 26% TFNs-D in Haining would first occur in 2020s with most flooding nodes concentrated on the northern part of Xishan road, and the remainder primarily distributed on Haining first avenue and Lianhe road. Most TFNs-D (31%) would first see dangerous level in 2060s. Under SSP2–4.5 scenario, much more places would experience the urban drainage pressure earlier in 2050s. Under SSP3–7.0, more than half TFNs-D (65%) would first see dangerous level during 2020s. Under the most severe

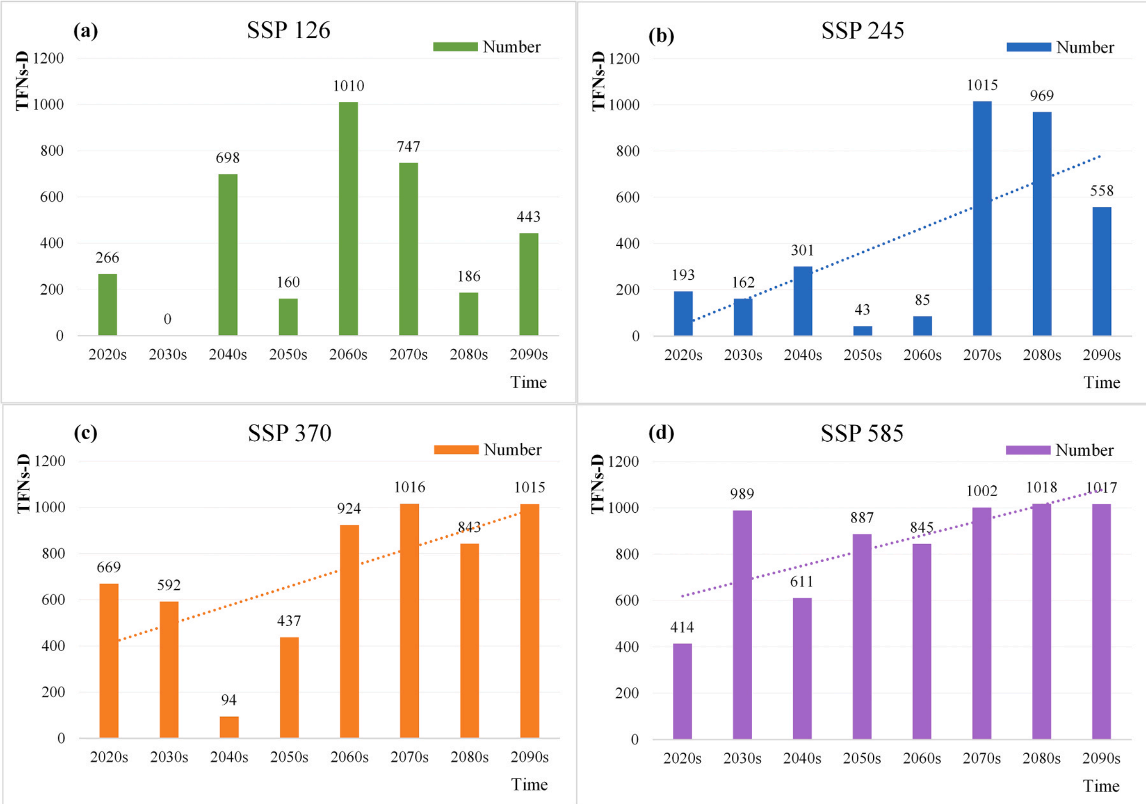

Fig. 7. The total number of flooding nodes with dangerous pressure level in each decade under four SSP-RCP scenarios: (a) SSP1-2.6, (b) SSP2-4.5, (c) SSP3-7.0, and (d) SSP5-8.5.

scenario, SSP5–8.5 in Fig. 8d, almost all the TFNs-D would first occur in earlier years during 2020s (41%) and 2030s (56%).

3.4.2. Changes in the duration of dangerous pressure

The percentage of duration of dangerous pressure under different SSP-RCP scenarios shows in Fig. 9. As emissions scenarios shift from SSP1–2.6 to SSP5–8.5, the percentage of duration over dangerous pressure would increase significantly. Under SSP1–2.6 scenario, the max percentage of duration over dangerous pressure would be one decade (26%). Three-decade duration over dangerous pressure would be the majority (38%) under SSP2–4.5 scenario, while around 33% of nodes experiencing dangerous pressure would last for seven decades. Under SSP5–8.5 scenario, the maximum percentage (40%) over dangerous pressure would be eight-decade duration.

The percentage of eight-decade duration would first occur under SSP2–4.5 scenario (8%), which were predicted to mainly distribute in the old resident area near Youquan road (Fig. 10b). Then, this percentage would increase to 9% under scenario SSP3–7.0 and 40% under SSP5–8.5 scenario, primarily scattered in Xishan road and Haining first avenue (Fig. 10c-d). In the case of SSP5–8.5 scenario, the dangerous duration of eight decades would occur in 60% nodes on Haining first avenue as shown in Fig. 10d. The maximum increase of 56% would happen over the 2080s and 2090s under SSP5–8.5 scenario, which are mainly distributed on Xishan roads.

4. Discussions

4.1. Explanations of urban drainage pressure changes under different SSP-RCP scenarios

Changes in precipitation extremes contribute much to the changes of urban drainage pressure. There would be more precipitation under the SSP5–8.5 scenario than the SSP1–2.6 scenario after 2060 (Tian et al., 2021). In the coming three decades, the precipitation would not change significantly relative to the baseline level. In the Yangtze River and Southeast River basins, the precipitation in the 2010s was lower than that during 1961–2010 (-6.53% to −0.06%) under different SPPs (Tian et al., 2021). The reason for this trend can be attributed to the two-stage evolution of the monsoon circulation between 2010 and 2099, characterized by a significant increase occurring after the 2040s. Across different SSP-RCP scenarios, urban flood volume would vary with precipitation levels. Generally, based on the current drainage system, larger precipitation extremes would result in greater TFV, which is in agreement with previous

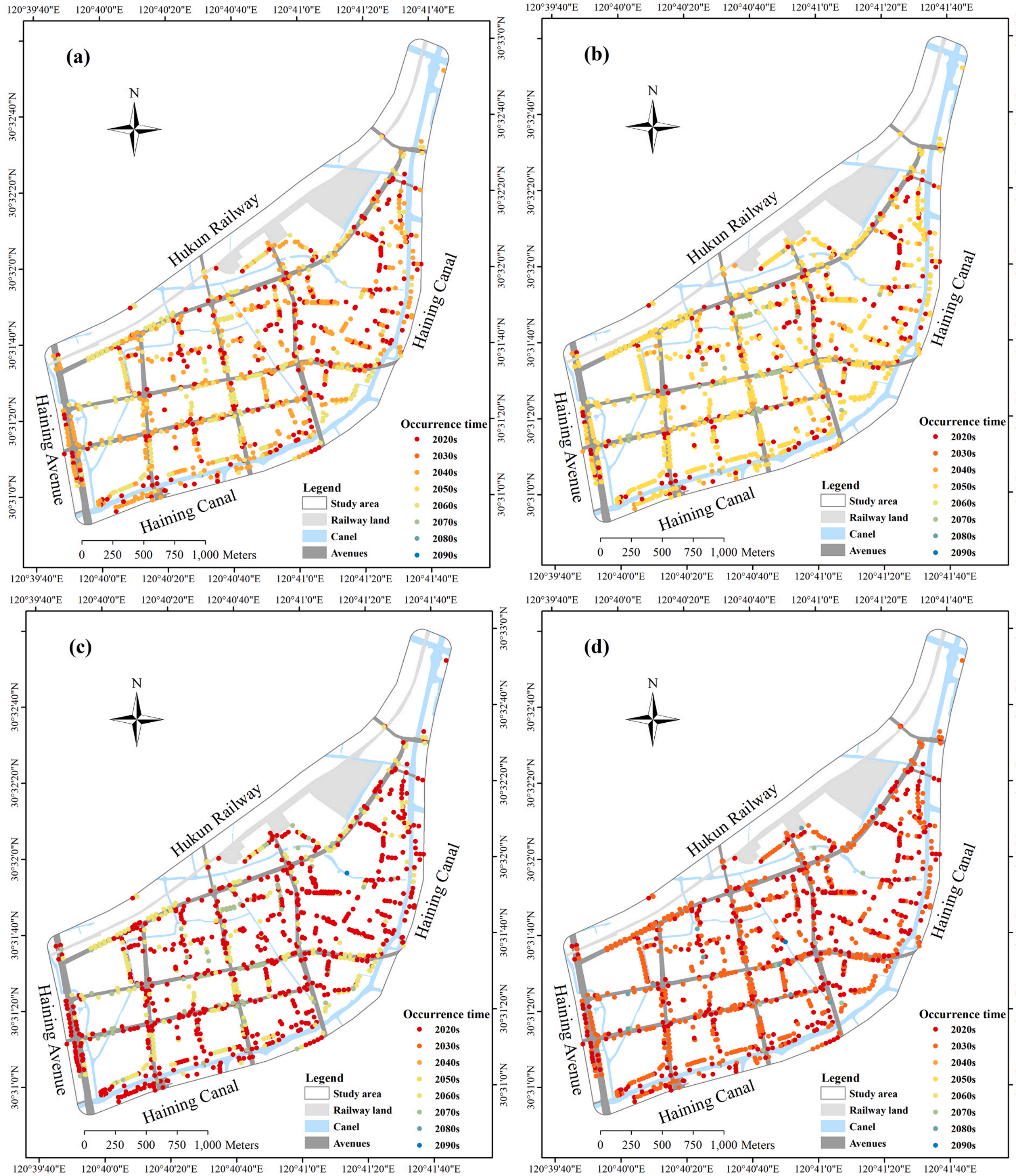

Fig. 8. The occurrence of dangerous pressure in the 21st century under four SSP-RCP scenarios: (a) SSP1-2.6, (b) SSP2-4.5, (c) SSP3-7.0, (d) SSP5-8.5.

findings (Li et al., 2022, Tabari, 2020). But specifically, the percent of TFNs would not show significant changes with precipitation. This could indicate that not all the areas would be sensitive to increase of precipitation extremes and the flood volume would be concentrated in specific areas (Ho et al., 2022, Wasko al., 2021). Therefore, it is necessary to assess the drainage system in sensitive area to upgrade or redesign the drainage infrastructure and ensure that it can meets the necessary standards.

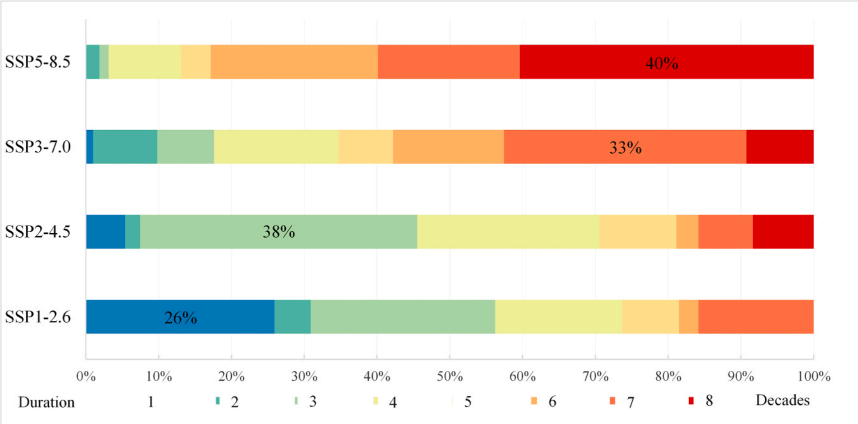

Fig. 9. Percentages of duration over dangerous pressure.

4.2. Indications on critical time points and high risk areas

Given that urban drainage pressure would increase significantly, it is apparent that the capacity of the present-day drainage system is insufficient to cope with the mounting urban drainage demands. Furthermore, the overarching urban drainage pressure trends in Haining suggest a consistent upward trajectory across various SSP-RCP scenarios with time. The critical period, characterized by the first reach of dangerous levels of urban drainage pressure, is projected to occur between the 2030s and 2050s, which aligns with the findings reported by Zhou et al. (2018). It should be noted that in scenarios with lower emissions, the critical point in time is anticipated to be delayed, occurring at a relatively later stage. This is due to more precipitation under the SSP5–8.5 scenario than the other scenario, which is also supported by the findings by Tian et al. (2021). The high risk areas are mainly located in Haining First Avenue, Xishan Road, and the old residential area in Fig. 1. The Haining first avenue would have high drainage pressure due to its low terrain and high percentage impervious area. In the Xishan road with limited drainage capacity in several manhole and the old residential part (e.g., the northern part of study area near Youquan road), the nodes would reach dangerous levels first and remain so for the longest time. In these areas, drainage facilities are constructed about 50 years ago which cannot meet the current drainage standards. Therefore, specific adaptations should be implemented, such as enlarging the pipes and conducting maintenance on the older pipes (Li et al., 2019; Neupane et al., 2021).

4.3. Limitations and future perspectives

The uncertainties mainly arise from GCMs, climate downscaling approach, SWMM model structure and parameter inputs in this study. Due to the unavailability of future sub-hourly climate projections, it was assumed that the regional storm intensity formula would remain constant in the future. Although we used five climate models to capture a wide range of climate variability, the full range may still not have been adequately represented (Du et al., 2022). Generally, the modelling outcomes indicate the potential primary impacts of climate change on urban floods. To obtain more robust results, the attention should be given to representing dynamic changes in rainfall patterns at hourly time level, while taking into account the non-stationary effects of climate change. Despite the given limitations, this study distinguishes itself from previous assessment studies, related to the critical time and hot spots of urban drainage pressure under various SSP-RCP scenarios using CMIP6 models. To provide a more comprehensive analysis, a two-dimensional surface flooding approach will be used to assess flood damage and risk.

5. Conclusions

Based on a combination of the climate projections by CMIP6 models and simulations by the SWMM model, this study takes Haining City as an example to assess the impact of future climate change on urban drainage pressure, determine critical periods, and identify high-risk areas. The main findings are as follows.

3121) Under different SSP-RCP scenarios caused by human activities, precipitation extremes would significantly increase particularly during the latter half of this century, with the SSP5–8.5 scenario representing the most severe case. Under SSP5–8.5 scenario, the urban flood volume would increase over 37% from the 2020s to the 2090s., and more than 97% of the flooding nodes would surpass the dangerous level by the 2030s.

3122) The critical time period for the initial occurrence of dangerous levels is projected to range from the 2030s to the 2050s. In instances of lower emission scenarios, the critical time point is expected to occur at a relatively later stage. The higher forcing pathway (SSP5–8.5) is expected to result in a notable increase in the proportion of nodes that initially exceed the critical

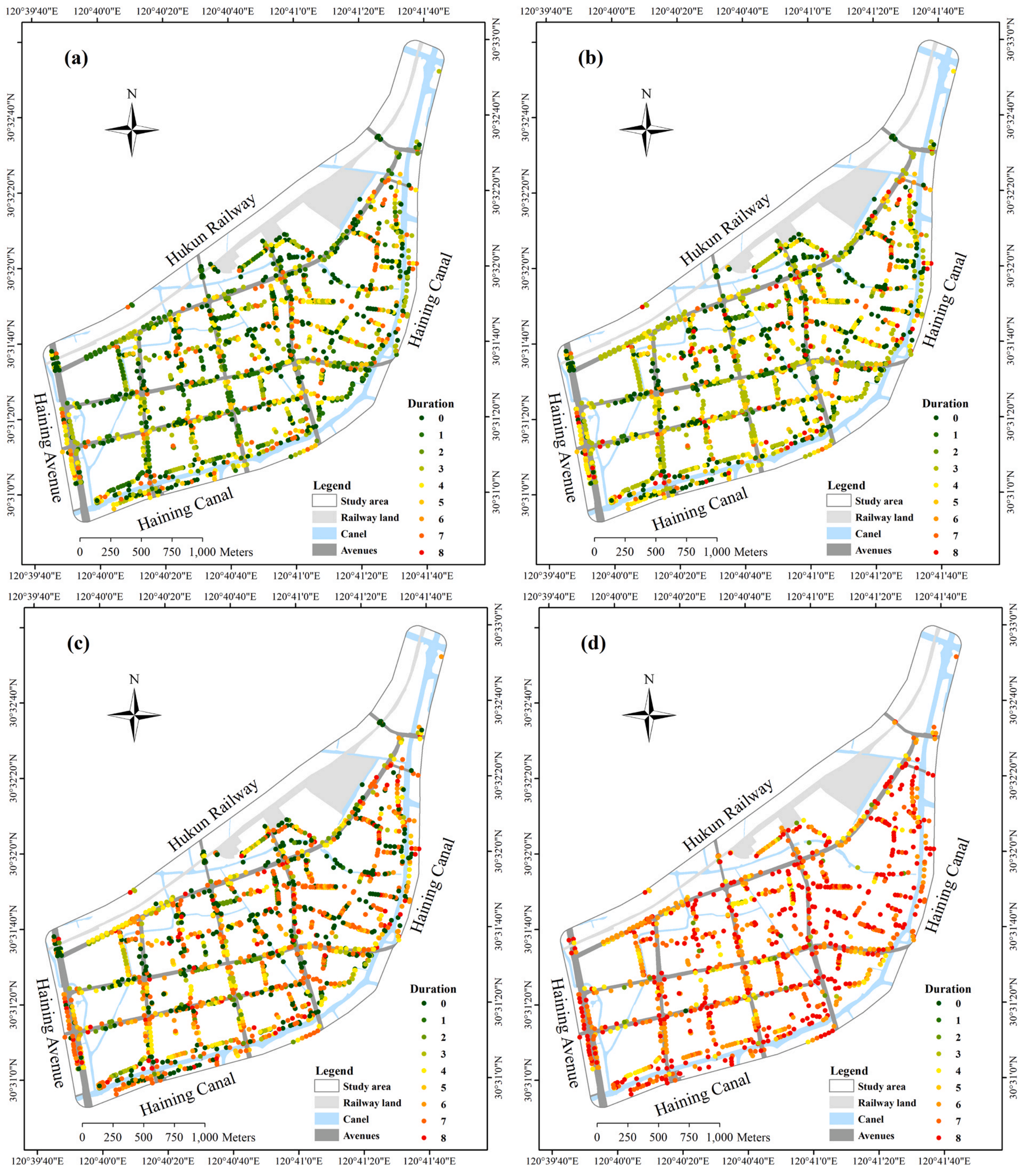

Fig. 10. The duration of dangerous pressure in 21st century under four SSP-RCP scenarios: (a) SSP1-2.6, (b) SSP2-4.5, (c) SSP3-7.0, (d) SSP5-8.5.

pressure level within the coming two decades, compared to the scenarios of SPP1–2.4, SPP2–4.5, and SPP3–7.0. Moreover, this scenario would cause about 40% of the nodes with dangerous pressure lasting for eight decades.

3123) The high risk areas are identified in Haining First Avenue, Xishan Road, and the old residential area, characterized by lower DEM and high intensity of building. Under the SSP5–8.5 scenario, it is projected that the duration of hazardous pressure spanning eight decades would impact 60% of nodes on Haining First Avenue. Along Xishan Road, the urban drainage pressure is expected to see a maximum increase of 56% during this century.

This study provides the first basis for identification of critical decades and high-risk areas of urban drainage pressure changes under future climate. This comprehensive analysis is expected to provide valuable insights for similar cities facing significant drainage capacity limitations. To provide a more comprehensive analysis, a two-dimensional surface flooding approach could be used to assess flood damage.

CRediT authorship contribution statement

Yao Li: Writing-original draft, Conceptualization, Methodology. **Pin Wang:** Conceptualization, Writing-review & editing. **Yihan Lou:** Investigation, Visualization. **Chaohui Chen:** Data curation. **Chenghua Shen:** Data curation. **Tangao Hu:** Writing-review & editing.

Declaration of Competing Interest

The authors declare that they have no known competing financial interests or personal relationships that could have appeared to influence the work reported in this paper.

Data availability

Data will be made available on request.

Acknowledgement

This work was supported by the National Natural Science Foundation of China (Grant No. 41807506), Zhejiang Provincial Natural Science Foundation of China (Grant No. LQ18D010007).

References

Bal, M., Dandpat, A.K., Naik, B., 2021. Hydrological modeling with respect to impact of land-use and land-cover change on the runoff dynamics in Budhabalanga river basing using ArcGIS and SWAT model. Remote Sens. Appl.: Soc. Environ. *23*, 100527.
Bibi, T.S., 2022. Modeling urban stormwater management in the town of Dodola based on landuse and climate change using SWMM 5.1. J. Hydrol.: Reg. Stud. *44*, 101267.
Blöschl, G., Hall, J., Viglione, A., Perdigão, R.A., Parajka, J., Merz, B., et al., 2019. Changing climate both increases and decreases European river floods. Nature 573 (7772), 108–111.
Chen, H., Sun, J., Lin, W., Xu, H., 2020. Comparison of CMIP6 and CMIP5 models in simulating climate extremes. Sci. Bull. 65 (17), 1415–1418.
China Statistical Yearbook, 2015. National Bureau of Statistics of China. China Statistics Press, Beijing, China.
Cos, J., Doblas-Reyes, F., Jury, M., Marcos, R., Bretonnière, P.A., Samsó, M., 2022. The Mediterranean climate change hotspot in the CMIP5 and CMIP6 projections. Earth Syst. Dyn. 13 (1), 321–340.
Dawkins, L.C., Osborne, J.M., Economou, T., Darch, G.J., Stoner, O.R., 2022. The advanced meteorology explorer: a novel stochastic, gridded daily rainfall generator. J. Hydrol., 127478
Depietri, Y., McPhearson, T., 2018. Changing urban risk: 140 years of climatic hazards in New York City. Clim. Change 148 (1), 95–108.
Du, Y., Wang, D., Zhu, J., Wang, D., Qi, X., Cai, J., 2022. Comprehensive assessment of CMIP5 and CMIP6 models in simulating and projecting precipitation over the global land. Int. J. Climatol. *42* (13), 6859–6875.
Eyring, V., Bony, S., Meehl, G.A., Senior, C.A., Stevens, B., Stouffer, R.J., Taylor, K.E., 2016. Overview of the coupled model intercomparison project phase 6 (CMIP6) experimental design and organization. Geosci. Model Dev. 9 (5), 1937–1958.
Farina, A., Di Nardo, A., Gargano, R., van der Werf, J.A., Greco, R., 2023. A simplified approach for the hydrological simulation of Urban Drainage Systems with SWMM. J. Hydrol., 129757
Gimenez-Maranges, M., Breuste, J., Hof, A., 2020. Sustainable Drainage Systems for transitioning to sustainable urban flood management in the European Union: A review. J. Clean. Prod. 255, 120191.
Guo, L., Jiang, Z., Chen, D., Le Treut, H., Li, L., 2020. Projected precipitation changes over China for global warming levels at 1.5° C and 2° C in an ensemble of regional climate simulations: impact of bias correction methods. Clim. Change 162, 623–643.
Heinze, C., Eyring, V., Friedlingstein, P., Jones, C., Balkanski, Y., Collins, W., Vancoppenolle, M., 2019. ESD Reviews: Climate feedbacks in the Earth system and prospects for their evaluation. Earth Syst. Dyn. 10 (3), 379–452.
Ho, M., Nathan, R., Wasko, C., Vogel, E., Sharma, A., 2022. Projecting changes in flood event runoff coefficients under climate change. J. Hydrol. 615, 128689.
Hou, J., Zhang, Y., Xia, J., Wang, Y., Zhang, S., Pan, X., Dou, M., 2022. Simulation and assessment of projected climate change impacts on urban flood events: Insights from flooding characteristic metrics. J. Geophys. Res.: Atmosp. *127* (3) e2021JD035360.
Kim, Y., Eisenberg, D., Bondank, E., Chester, M., Mascaro, G., Underwood, B., 2017. Fail-safe and safe-to-fail adaptation: decision-making for urban flooding under climate change. Clim. Change 145 (3), 397–412.
Li, J., Bortolot, Z.J., 2022. Quantifying the impacts of land cover change on catchment-scale urban flooding by classifying aerial images. J. Clean. Prod. *344*, 130992.
Li, Y., Hu, T., Zheng, G., Shen, L., Fan, J., Zhang, D., 2019. An Improved Simplified Urban Storm Inundation Model Based on Urban Terrain and Catchment Modification. Water 11 (11), 2335.
Li, Y., Huang, J.J., Hu, M., Yang, H., Tanaka, K., 2020. Design of low impact development in the urban context considering hydrological performance and life-cycle cost. J. Flood Risk Manag. *13* (3), e12625.
Li, Y., Osei, F.B., Hu, T., Stein, A., 2022. Urban flood susceptibility mapping based on social media data in Chengdu city, China. Sustain. Cities Soc., 104307
Lisenbee, W.A., Hathaway, J.M., Winston, R.J., 2022. Modeling bioretention hydrology: Quantifying the performance of DRAINMOD-Urban and the SWMM LID module. J. Hydrol. 612, 128179.
Liu, W., Feng, Q., Engel, B.A., Yu, T., Zhang, X., Qian, Y., 2023. A probabilistic assessment of urban flood risk and impacts of future climate change. J. Hydrol., 129267
Lou, Y., Wang, P., Li, Y., Wang, L., Chen, C., Li, J., Hu, T., 2024. Management of the designed risk level of urban drainage system in the future: Evidence from haining city, China. J. Environ. Manag. 351, 119846.
Lu, Y., Yan, Y., Ding, D., Zhao, C., Song, Y., Zhao, J., 2018. Trends of extreme precipitation in China and their influence on urban drainage pressure. Acta Ecol. Sin. 38 (5), 1661–1667.
Luo, K., Zhang, X., 2022. Increasing urban flood risk in China over recent 40 years induced by LUCC. Landsc. Urban Plan. 219, 104–317.

Moustakis, Y., Papalexiou, S.M., Onof, C.J., Paschalis, A., 2021. Seasonality, intensity, and duration of rainfall extremes change in a warmer climate. Earth'S. Future 9 e2020EF001824.
NCC-Editorial, 2019. The CMIP6 landscape. Nat. Clim. Change 9, 727-727.
Neupane, B., Vu, T.M., Mishra, A.K., 2021. Evaluation of land-use, climate change, and low-impact development practices on urban flooding. Hydrol. Sci. J. *66* (12), 1729–1742.
O'Neill, B.C., Tebaldi, C., Van Vuuren, D.P., Eyring, V., Friedlingstein, P., Hurtt, G., Sanderson, B.M., 2016. The scenario model intercomparison project (ScenarioMIP) for CMIP6. Geosci. Model Dev. 9 (9), 3461–3482.
Piao, J., Chen, W., Wang, L., Chen, S., 2022. Future projections of precipitation, surface temperatures and drought events over the monsoon transitional zone in China from bias-corrected CMIP6 models. Int. J. Climatol. 42 (2), 1203–1219.
Rossman, L.A., 2015. Storm water management model user's manual, version 5.1. National Risk Management Research Laboratory, Office of Research and Development, US Environmental Protection Agency, Cincinnati.
Son, Y., Di Lorenzo, E., Luo, J., 2023. WRF-Hydro-CUFA: A scalable and adaptable coastal-urban flood model based on the WRF-Hydro and SWMM models. Environ. Model. Softw. 167, 105770.
Sun, X., Li, R., Shan, X., Xu, H., Wang, J., 2021. Assessment of climate change impacts and urban flood management schemes in central Shanghai. Int. J. Disaster Risk Reduct. 65, 102563.
Tabari, H., 2020. Climate change impact on flood and extreme precipitation increases with water availability. Sci. Rep. *10* (1), 1–10.
Tang, Z., Wang, P., Li, Y., Sheng, Y., Wang, B., Popovych, N., Hu, T., 2024. Contributions of climate change and urbanization to urban flood hazard changes in China's 293 major cities since 1980. Journal of Environmental Management 353, 120113.
Tebaldi, C., Debeire, K., Eyring, V., Fischer, E., Fyfe, J., Friedlingstein, P., Ziehn, T., 2020. Climate model projections from the scenario model intercomparison project (ScenarioMIP) of CMIP6. Earth Syst. Dyn. Discuss. 2020, 1–50.
Tellman, B., Sullivan, J., Kuhn, C., Kettner, A., Doyle, C., Brakenridge, G., et al., 2021. Satellite imaging reveals increased proportion of population exposed to floods. Nature 596 (7870), 80–86.
Tian, J., Zhang, Z., Ahmed, Z., Zhang, L., Su, B., Tao, H., Jiang, T., 2021. Projections of precipitation over China based on CMIP6 models. Stoch. Environ. Res. Risk Assess. 35 (4), 831–848.
Wang, L., Chen, W., 2013. Application of bias correction and spatial disaggregation in removing model biases and downscaling over China. Adv. Earth Sci. 28 (10), 1144.
Wang, L., Li, Y., Hou, H., Chen, Y., Fan, J., Wang, P., Hu, T., 2022. Analyzing spatial variance of urban waterlogging disaster at multiple scales based on a hydrological and hydrodynamic model. Nat. Hazards 114 (2), 1915–1938.
Wang, P., Li, Y., Fan, J., Kong, F., Zhang, D., Hu, T., 2023. Future changes in urban drainage pressure caused by precipitation extremes in 285 cities across China based on CMIP6 models. Sustain. Cities Soc. 91, 104404.
Wasko, C., Nathan, R., Stein, L., O'Shea, D., 2021. Evidence of shorter more extreme rainfalls and increased flood variability under climate change. J. Hydrol. 603, 126994.
Wetterhall, F., Bárdossy, A., Chen, D., Halldin, S., Xu, C.Y., 2006. Daily precipitation-downscaling techniques in three Chinese regions. Water Resour. Res. 42, 11.
Xu, H., Chen, H., Wang, H., 2022. Future changes in precipitation extremes across China based on CMIP6 models. Int. J. Climatol. 42 (1), 635–651.
Yang, Y., Li, J., Huang, Q., Xia, J., Li, J., Liu, D., Tan, Q., 2021. Performance assessment of sponge city infrastructure on stormwater outflows using isochrone and SWMM models. J. Hydrol. 597, 126151.
Zhai, R., Tao, F., Lall, U., Fu, B., Elliott, J., Jägermeyr, J., 2020. Larger drought and flood hazards and adverse impacts on population and economic productivity under 2.0 than 1.5°C warming. Earth'S. Future 8 e2019EF001398.
Zhang, W., Li, T., 2015. The influence of objective function and acceptability threshold on uncertainty assessment of an urban drainage hydraulic model with generalized likelihood uncertainty estimation methodology. Water Resour. Manag. 29, 2059–2072.
Zhou, Q., Leng, G., Huang, M., 2018. Impacts of future climate change on urban flood volumes in Hohhot in northern China: benefits of climate change mitigation and adaptations. Hydrol. Earth Syst. Sci. 22 (1), 305–316.
Zhou, Q., Leng, G., Su, J., Ren, Y., 2019. Comparison of urbanization and climate change impacts on urban flood volumes: Importance of urban planning and drainage adaptation. Sci. Total Environ. 658, 24–33.
Zhu, Y., Xu, C., Liu, Z., Yin, D., Jia, H., Guan, Y., 2023. Spatial layout optimization of green infrastructure based on life-cycle multi-objective optimization algorithm and SWMM model. Resour., Conserv. Recycl. *191*, 106906.
Zhuang, Q., Li, M., Lu, Z., 2023. Assessing runoff control of low impact development in Hong Kong's dense community with reliable SWMM setup and calibration. J. Environ. Manag. 345, 118599.